Biomaterials 85 (2016) 232–245

Contents lists available at ScienceDirect

Biomaterials

journal homepage: www.elsevier.com/locate/biomaterials

Synergistic anti-tumor activity through combinational intratumoral injection of an in-situ injectable drug depot

Da Yeon Kim [a], Doo Yeon Kwon [a], Jin Seon Kwon [a], Ji Hoon Park [a], Seung Hun Park [a], Hyun Ju Oh [a], Jae Ho Kim [a], Byoung Hyun Min [a], Kinam Park [b], Moon Suk Kim [a, *]

[a] Department of Molecular Science and Technology, Ajou University, Suwon, 443-759, Republic of Korea
[b] Departments of Biomedical Engineering and Pharmaceutics, Purdue University, IN 47907-1791, USA

ARTICLE INFO

Article history:
Received 9 October 2015
Received in revised form
19 January 2016
Accepted 1 February 2016
Available online 2 February 2016

Keywords:
Tumors
Doxorubicin
5-Fluorouracil
Intratumoral injection
Injectable depot

ABSTRACT

Here, we describe combinational chemotherapy via intratumoral injection of doxorubicin (Dox) and 5-fluorouracil (Fu) to enhance the efficacy and reduce the toxicity of systemically administered Fu and Dox in cancer patients. As the key concept in this work, mixture formulations of Dox-loaded microcapsules (Dox-M) and Fu-loaded Pluronic® hydrogels (Fu-HP) or Fu-loaded diblock copolymer hydrogels (Fu-HC) have been employed as drug depots. The *in vitro* and *in vivo* drug depot was designed as a formulation of Dox-M dispersed inside an outer shell of Fu-HP or Fu-HC after injection. The Dox-M/Fu-HP and Dox-M/Fu-HC formulations are free flowing at room temperature, indicating injectability, and formed a structural gelatinous depot *in vitro* and *in vivo* at body temperature. The Fu-HP, Fu-HC, Dox-M/Fu-HP, Dox-M/Fu-HC, and Dox-M formulations were easily injected into tumor centers in mice using a needle. Dox-M/Fu-HC produced more significant inhibitory effects against tumor growth than that by Dox-M/Fu-HP, while Fu-HP, Fu-HC and Dox-M had the weakest inhibitory effects of the tested treatments. The *in vivo* study of Dox and Fu biodistribution showed that high Dox and Fu concentrations were maintained in the target tumor only, while distribution to normal tissues was not observed, indicating that Dox and Fu concentrations below their toxic plasma concentrations should not cause significant systemic toxicity. The Dox-M/Fu-HP and Dox-M/Fu-HC drug depots described in this work showed excellent performance as chemotherapeutic delivery systems. The results reported here indicate that intratumoral injection using combination chemotherapy with Dox-M/Fu-HP or Dox-M/Fu-HC could be of translational research by enhancing the synergistic inhibitory effects of Dox and Fu on tumor growth, while reducing their systemic toxicity in cancer patients.

© 2016 Elsevier Ltd. All rights reserved.

1. Introduction

As a first treatment, most cancer patients receive surgery to remove as much of the tumor as possible [1]. Thereafter, systemic chemotherapy or local radiotherapy is performed to eliminate residual cancer and prevent the recurrence of carcinogenesiss [2].

Many chemotherapeutic drugs have been used clinically. Doxorubicin (Dox) and 5-fluorouracil (Fu) have been extensively employed in individual and combinational chemotherapy for solid tumors [3–5]. Because both Dox and Fu can effectively treat many types of solid tumors, we hypothesized that cancer treatment with a combination of Dox and Fu could synergistically inhibit tumor growth *in vivo*.

However, it is difficult to achieve drug accumulation inside the target tumor with drug-only formulations of Dox and Fu owing to rapid clearance from tumor by the blood circulation [6,7]. Furthermore, reports have found that drug-only formulations of Dox and Fu showed *in vivo* stability for up to 1 day or a few days, respectively [8–10]. Thus, repeated administration of Dox and Fu is required to maintain therapeutic activity at target tumors [11]. However, numerous studies have found that administration of Dox or Fu can cause side effect owing to low selective chemotherapeutics through dose-limiting of the drugs [12].

Therefore, maintenance of therapeutic concentrations of Dox and Fu within target tumor tissues over a prolonged period with few systemic side effects has been the goal of most researches (Fig. 1).

Targeted drug delivery, such as direct intratumoral injection, can

* Corresponding author. Tel.: +82 31 219 2608; fax: +82 31 219 3931.
E-mail address: moonskim@ajou.ac.kr (M.S. Kim).

http://dx.doi.org/10.1016/j.biomaterials.2016.02.001
0142-9612/© 2016 Elsevier Ltd. All rights reserved.

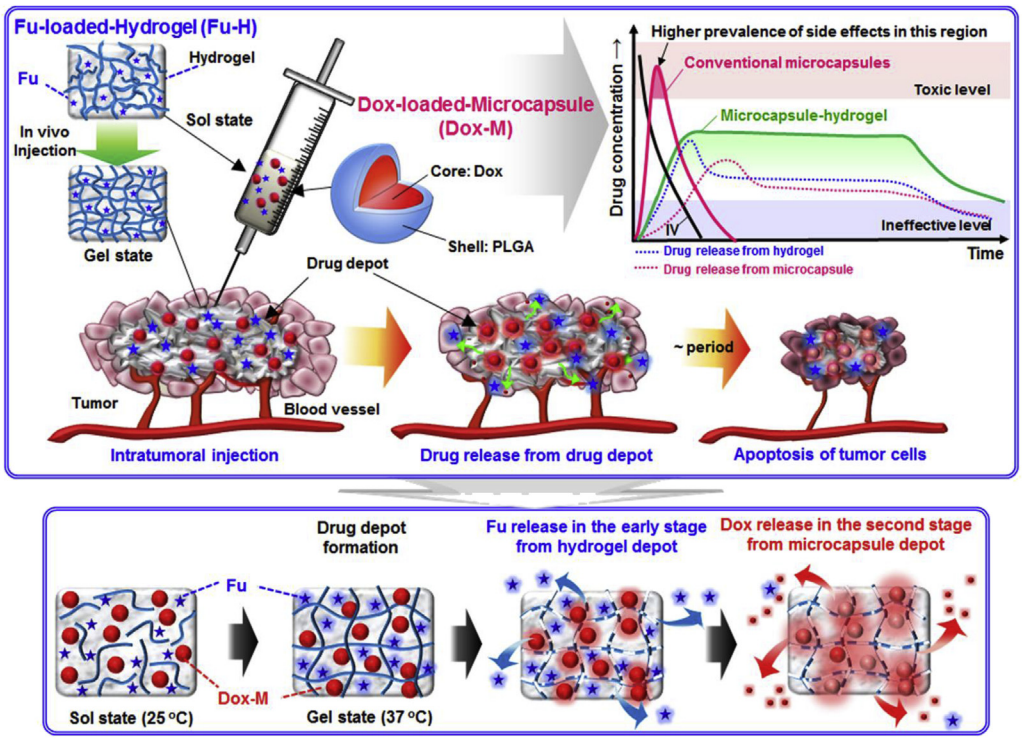

Fig. 1. Schematic representation of synergistic tumor suppression via intratumoral injections of dual-drug depots and controlled release of Dox and Fu in the first and second stage.

achieve a high local concentration inside the target tumor. In addition, injectable depot formulations of Dox or Fu can greatly increase desirable outcomes while minimizing negative side effects. It is therefore feasible that direct target delivery of injectable depot formulations of Dox or Fu could be achieved by intratumoral injection.

During the last decade, injectable in situ-forming hydrogels have attracted considerable attention, because they can exhibit solution-to-gel phase transition in response to changes in temperature [13,14]. Various anticancer drugs can be incorporated easily into the hydrogel solution at room temperature by simple mixing. Anticancer drug-loaded hydrogel (DH) solutions form hydrogel depots *in situ* at site-specific positions under physiological conditions, resulting in prolonged action periods for the loaded anticancer drugs.

Recently, our group reported a biodegradable poly(ethylene glycol)-*b*-poly(caprolactone-co-lactide) diblock copolymer (HC) as an intratumorally injectable drug depot with a biodegradation window adjustable from a few weeks to a few months [15–17]. Application of HC for intratumoral chemotherapy represents a promising approach to maintain therapeutic concentrations of Dox and Fu within the tumor through a single injection, as well as to induce biodegradation of the drug depot over a defined treatment period.

Microencapsulation has the capacity to selectively entrap a particular drug in a polymer matrix. Drug-loaded microcapsules (DM) can be subcutaneously or intratumorally injected to form a drug depot, where they slowly release their drug contents over time. Thus, DM depots can significantly reduce dosage frequency and improve drug efficacy without increasing the risk of toxicity. In previous studies, our group manufactured DM using a mono-axial nozzle ultrasonic atomizer [18–20]. Several drugs were encapsulated in the inner core of the microcapsules. Microcapsules with a round shape formed a DM depot following subcutaneous injection. In addition, *in vivo* drug release from the DM depot was maintained for at least 4 weeks in rats.

Because both DH and DM formulations can be easily prepared as solution and then can form drug depot through minimally invasive chemotherapeutic administration, thus we believed that intratumoral injection of a combination of anticancer DH and DM would effectively inhibit tumor growth.

To the best of our knowledge, intratumoral injection of combinations of DH and DM with anticancer drugs into animals has received little study for *in vivo* cancer treatment. Thus, in this work developing an efficient *in vivo* delivery strategy of combination of drug depot can achieve an unmet need for cancer treatment.

The *first aim of this work* was to prepare combination formulation of DH and DM with Dox and Fu (Fig. 1). Based on the stability of Dox and Fu, Dox (with 1 week of stability) was encapsulated inside the inner core of the Dox microcapsules (Dox-M) to prolong its action period, while Fu (with a few weeks of stability) was loaded in the in-situ hydrogels (Fu-H). Because the Fu-H was a viscous solution at room temperature, the easiest method of preparing the injectable Dox-M/Fu-H depot was to simply mix the Dox-M into the Fu-H solution. Thus, the Dox-M/Fu-H drug depot could be formulated with Dox-M dispersed inside an outer shell of Fu-H. It was expected that utilizing the microcapsule and hydrogel forms of Dox and Fu, respectively, would control their release. In addition, the hydrogel acts as an outer shell for the Dox-M, resulting in sustained Dox release from the microcapsules.

Reports have shown that the properties of hydrogels control the release of encapsulated drugs [18,21]. Recently, our group reported that Pluronic® and HC hydrogels showed a gel persistence of 2 days and a few weeks, respectively, and accordingly showed different drug release patterns [22]. Thus, in this work, we assessed the release of Fu and Dox from Dox-M/Fu-HP and Dox-M/Fu-HC prepared by using Pluronic® and HC with different gel persistence times, respectively, as additional outer shells. The *second aim of this work* was to compare the effects of Dox-M/Fu-HP and Dox-M/Fu-HC on tumor growth.

Accordingly, the overall aim of this study was to assess *in vivo* intratumoral injection of Dox-M/Fu-HP and Dox-M/Fu-HC in comparison with Dox-M in the context of the following specific goals: 1) to evaluate whether the prepared injectable formulations of Dox-M/Fu-HP and Dox-M/Fu-HC can be intratumorally injected to produce drug depots, (2) to determine whether the injectable formulations produce a synergistic inhibitory effect on tumor growth in comparison with Dox-M. These studies were conducted with the goal of providing a rationale for tumor treatment through combination therapy with Dox-M/Fu-HP and Dox-M/Fu-HC.

2. Materials and methods

2.1. Materials

Low molecular weight PLGA (lactic/glycolic acid: 50/50; MW: 33,000 Da) was purchased from Birmingham Polymers, Inc. (Birmingham, AL, USA). Poly(vinyl alcohol) (PVA; 87–89% hydrolyzed; MW: 85,000–124,000 Da) was purchased from Sigma–Aldrich (St. Louis, MO, USA) and used as an emulsifier. Dox and Fu were purchased from Wako Pure Chemical (Tokyo, Japan). Pluronic® F-127 was used as received from BASF SE (Ludwigshafen, Germany). All other chemicals were of analytical grade and used without further purification.

2.2. Preparation of Dox-M

Microcapsules were generated using a mono-axial nozzle ultrasonic atomizer (Sono-Tek Corp, Milton, NY, USA). The Dox-M was prepared as follows: a PLGA solution in ethyl acetate and an aqueous solution containing Dox were separately fed into an ultrasonic atomizer. The flow rates of the PLGA solution (3% w/v) and Dox aqueous solution (4% w/v) were 4 and 0.2 mL/min, respectively. Atomization of the mixed solution of PLGA and Dox was performed for approximately 5 s at a vibration frequency of 3 W/60 kHz to produce microdroplets. The distance between the atomizer head and aqueous PVA solution was 1 cm. The stirring speed of the PVA solution was 1000 rpm. The resulting solutions were gently stirred for 2 h in a 0.5% w/v PVA solution to allow solidification of the microcapsules and washed with distilled water. The solution was frozen at −74 °C, followed by freeze-drying over 4 days.

2.3. Encapsulation efficiency of the Dox-M

To determine the encapsulation efficiency of Dox inside the Dox-M, 10 mg of the Dox-M was placed into a test tube. Next, 0.6 mL of CH_2Cl_2 was added to dissolve the polymer portion of the microcapsules, followed by the addition of 1.4 mL of DW to allow solubilization of the Dox. The resulting solution was sonicated for 90 min at 25 °C and centrifuged at 10,000 rpm for 5 min. The amount of Dox was determined using a high performance liquid chromatography (HPLC) system (Agilent 1200 series, Waldbronn, Germany). The HPLC was equipped with a detector operating at a wavelength of 470 nm and a CAPCELL PACK C18 column (5 μm, 4.6 × 250 mm, Shiseido Co., Ltd., Tokyo, Japan). The mobile phase consisted of a mixture of 50 mM sodium phosphate and acetonitrile (75:25, v/v). The column was eluted at a flow rate of 0.5 mL/min. Three independent release experiments were performed for the Dox-M. The encapsulation efficiency was determined using the following equation:

$$E(\%) = [(\text{amount of encapsulated Dox})/(\text{total amount of Dox added})] \times 100$$

2.4. Preparation of Fu-loaded HC (Fu-HC) and Fu-loaded HP (Fu-HP) hydrogels

MPEG-b-(PCL-ran-PLLA) (750-2420-90) (HC) was prepared using a block copolymerization method reported previously[15–17]. The HC copolymer was dissolved in phosphate-buffered saline (PBS) (pH 7.4) at 20% w/v in 5-mL vials and stirred at 70 °C. Fu (0.2 or 0.4 mg/mL) was added to the HC solution to prepare Fu-HC, which was stored at 4 °C for 48 h. For the Pluronic® (HP) solution, HP was dissolved in deionized water at 20% w/v in 5-mL vials at 0 °C. Fu (0.2 or 0.4 mg/mL) was added to the HP solution to prepare Fu-HP, which was stored at 4 °C for 48 h.

2.5. Preparation of the Dox-M/Fu-HC and Dox-M/Fu-HP mixtures

The prepared Dox-M (0.2 mg/mL Dox) was added to the Fu-HC and Fu-HP solutions (0.2 mg/mL Fu) and mixed to prepare the Dox-M/Fu-HC and Dox-M/Fu-HP formulations, respectively, which were stored at 4 °C for 48 h.

2.6. Viscosity and rheological measurements of injectable formulations

Firstly, viscosity was measured using a Brookfield Viscometer DV-III Ultra instrument with a programmable rheometer and a circulating bath with a programmable controller (TC-502P). The viscosity measurement was performed in the vessel using a tight cap to prevent evaporation of water from the samples of Dox-M alone, HP alone, HC alone, Fu-HP, Fu-HC, Dox-M/Fu-HP, and Dox-M/Fu-HC. The viscosities of all formulations were investigated using a T-F spindle rotating at 0.2 rpm at temperatures between 10 °C and 60 °C (raised in increments of 1 °C/2 min).

Next, rheological properties were measured using a modular compact rheometer (MCR 102, Anton Paar, Austria) with politer temperature controlled bottom platen. The parallel plate diameter used was 25 mm and the distance between the plates was 0.3 mm at room temperature and 37 °C. A frequency sweep was measured between 0.1 Hz and 10 Hz of the oscillating frequency at a strain of 2%. The strain sweep was measured between 0.1 and 100% of the oscillating strain at a constant frequency of 1 Hz. All rheological properties were analyzed with the instrument software (Rheoplus/32, version V3.21, Anton Paar, Austria).

2.7. In vitro release

Dox-M alone (0.4 mg Dox), Fu-HP (0.4 mg Fu), Fu-HC (0.4 mg Fu), Dox-M/Fu-HP (0.2 mg Dox, 0.2 mg Fu), and Dox-M/Fu-HC (0.2 mg Dox, 0.2 mg Fu) were transferred to fresh 5-mL vials, suspended in 4 mL of PBS (pH 7.4), and shaken at 100 rpm in an incubator at 37 °C. At the specified sample collection times, 0.5 mL of the solution was removed from each vial and replaced with 0.5 mL of fresh PBS (maintained at 37 °C).

The amount of Dox release was determined using HPLC as described Section 2.3. The amount of Fu release was determined

using HPLC at a wavelength of 260 nm and a column flow rate of 0.8 mL/min. The mobile phase consisted of a mixture of 50 mM sodium phosphate and acetonitrile (30:70, v/v). Four independent release experiments were performed for each sample. The cumulative amount of Dox and Fu released *in vitro* was calculated by comparison with standard calibration curves prepared with known concentrations of Dox and Fu.

2.8. In vitro antitumor activity

B16F10 melanoma cells (2×10^4 cells/well) were seeded in the lower chambers of a 24-well Transwell® plate (SPL Life Science, 0.4-μm pore size) and incubated for 1 day at 37 °C in a humidified incubator containing 5% CO_2. B16F10 melanoma cells were allowed to proliferate (3×10^6 cells/well) for tests of *in vitro* antitumor activity. PBS, free Dox (0.4 mg Dox/well), free Fu (0.4 mg Fu/well), free Dox and Fu (0.2 mg Dox, 0.2 mg Fu), and Dox-M alone (0.4 mg Dox) were added directly to the upper chambers of the Transwell® plate to examine the *in vitro* antitumor activity of these solutions against B16F10 cancer cells.

To create a drug depot, 150 μL of the Fu-HP (0.4 mg Fu/well), Fu-HC (0.4 mg Fu/well), Dox-M/Fu-HP (0.2 mg Dox and 0.2 mg Fu per well), or Dox-M/Fu-HC (0.2 mg Dox and 0.2 mg Fu per well) formulations were added to the upper chamber of the Transwell® plate and maintained at 37 °C in a humidified incubator for 1 h. Each upper chamber was placed above a lower chamber containing B16F10 cells (2×10^4 cells/well). Each Transwell® plate was maintained at 37 °C in a humidified incubator containing 5% CO_2.

For all formulations, the initial medium was changed after 12 h. After 12, 24, 48, and 72 h, the *in vitro* cytotoxicity of all formulations toward B16F10 cancer cells was compared using the MTT (3-(4,5-dimethylthiazol-2-yl)-2,5-diphenyltetrazolium bromide; Sigma–Aldrich Co., St. Louis, MO, USA) assay. In brief, 100 μL of PBS solution containing the MTT tetrazolium substrate (50 μg/mL) was added to each 96-well plate and the plates were incubated at 37 °C for 4 h. The resulting violet formazan precipitate was solubilized by the addition of 500 μL DMSO and shaken for 30 min. The solutions were placed in 96-well plates and read using a microplate reader (E-max, Molecular Devices, Sunnyvale, CA, USA). The optical density of each well was measured at a wavelength of 590 nm. All experiments were performed at least 4 times and the results were presented as mean ± standard deviation (SD).

2.9. In vitro fluorescent microscopy images

To obtain fluorescent microscopy images of B16F10 melanoma cells, cells in 24-well Transwell® plates were treated with PBS, Dox-M, Dox-M/Fu-HP, or Dox-M/Fu-HC as described in the previous section. B16F10 melanoma cells were incubated for 12, 24, 48, and 72 h and washed with minimal essential medium (MEM). Next, the B16F10 melanoma cells were treated with 500 mL of 5 μg/mL Hoechst 33324 solution (Invitrogen, Carlsbad, CA, USA) to stain the cell nuclei and incubated for 30 min at 37 °C in an atmosphere of 5% CO_2. Fluorescent images were obtained using an Olympus IX51 inverted fluorescence microscope (Olympus, Tokyo, Japan) and analyzed with Motic Images Advanced 3.2 software (Motic Co. Ltd., Hong Kong, China).

2.10. In vivo antitumor activity

The protocols of this study were approved by the Institutional Animal Experiment Committee (approval no. 2013-0065) of the School of Medicine of Ajou University. The *in vivo* experiments were carried out in accordance with the approved guidelines. The tumor model was established by subcutaneous inoculation of approximately 2×10^5 B16F10 melanoma cells (in a 100-μL suspension) into the abdomen of C57BL/6 mice (6-weeks-old, female, 17–20 g). The time at which the volume of the solid tumors reached 150–200 mm^3 was defined as day 0.

One hundred twenty C57BL/6 mice, divided randomly into 6 groups of 20 mice each, were used in the animal tests. The animals were assigned to 6 experimental groups: (1) normal saline, (2) Dox-M alone (0.4 mg Dox), (3) Fu-HP (0.4 mg Fu), (4) Fu-HC (0.4 mg Fu), (5) Dox-M/Fu-HP (0.2 mg Dox, 0.2 mg Fu), and (6) Dox-M/Fu-HC (0.2 mg Dox, 0.2 mg Fu). On day 0, 200 μL of each solution was intratumorally injected into the tumor using a 21-gauge needle on a disposable 1-mL syringe. The injection speed of each solution maintained the 10 μL/s to protect the over flow into the adjacent tissue spaces. Antitumor activity was assessed by measuring tumor diameters in 2 dimensions with Vernier calipers on predefined days. The tumor volume (V) was calculated according to the following formula: $V = [\text{length} \times (\text{width})^2]/2$.

For pharmacokinetics, experimental animals were scarified on days 1, 6, 12, and 18 following treatment by cervical dislocation. The organs (tumor, intestine, stomach, lung, kidney, liver, spleen, and heart) were harvested immediately from each animal. Images of the harvested organs were collected using a fluorescence imaging system (Dolan-Jenner PL-800 fiber optic illuminator; 150 W EKE quartz halogen light, glass reference number OG515 filter; Dolan-Jenner Industries, Boxborough, MA, USA). Fluorescence images were taken within a wavelength of 515 nm and at an excitation wavelength of 470 nm. After digitization using a charge-coupled device (CCD), fluorescence images were visualized with Axiovision Rel. 4.8 (Carl Zeiss Microimaging GmbH, Göttingen, Germany).

To determine the amounts of Dox and Fu remaining in the organs of the treated mice, each organ was homogenized in a 0.3N HCl/70% ethanol solution using T 10 basic ULTRA-TURRAX Homogenizer (IKA®-Werke GmbH & Co., Staufen, Germany) at 25,000–30,000 rpm for 10 min and incubated at 37 °C for 15 min. Each sample was mixed with an equal volume of 40% $ZnSO_4$ and the mobile phase (see Section 2.7), followed by re-incubation at 37 °C for 15 min. After centrifugation at 2000 rpm for 10 min, the amounts of Dox and Fu in the supernatant were calculated by reference to a standard calibration curve prepared from solutions containing known concentrations of Dox and Fu in the mobile phase. The amount of Dox and Fu in each organ was determined using HPLC as described in Section 2.7. Three independent experiments were performed for each organ.

To assess the *in vivo* biodegradability of HP and HC, 200 μL of solutions of HP and HC were injected subcutaneously into the dorsal parts of the mice, because it is not possible to separate the HP and HC from the intratumorally injected formulations containing HP and HC. The areas where HP and HC were administered were dissected after 18 days. Because HP completely disappeared after 2–3 days, CH_2Cl_2 (1 mL) was added to each tissue sample from the HC-treated mice in a test tube to dissolve the HC portion. Next, 1 mL of distilled water was added to solubilize the tissue. The resulting mixture was sonicated for 90 min at 25 °C and centrifuged at 10,000 rpm for 5 min. The CH_2Cl_2 solution was collected, CH_2Cl_2 was evaporated, and the remaining HC containing degraded compounds was freeze-dried until it reached a constant weight. The degraded compounds were measured by NMR.

To assess the Dox-M dispersed inside an outer shell of Fu-H, 200 μL of solutions of Dox-M/Fu-HC were injected subcutaneously into the dorsal parts of the mice. Dox-M/Fu-HC removed from the rat at 1 day was immediately mounted on a metal stub pre-cooled in liquid nitrogen. After mounting of the Dox-M/Fu-HC, the metal stub was quickly immersed in a liquid nitrogen bath to minimize alteration of the Dox-M/Fu-HC. The stub then was freeze-dried at −75 °C using a freeze dryer. Once completely dry, the

sample on the metal stub was coated with a thin layer of gold using a plasma sputtering apparatus (Ted Pella, Cressington 108 Auto, CA, USA) under an argon atmosphere. The Dox-M/Fu-HC was also examined by scanning electron microscopy (SEM) using a JSM-6380 SEM (JEOL, Tokyo, Japan).

2.11. Histological analysis

On days 1, 6, 12, and 18 after injection, mice were sacrificed and the tumors were individually dissected and removed from the subcutaneous area of the abdomen. The tumor tissue samples were immediately fixed with 10% formalin and embedded in paraffin. The embedded specimens were sectioned (4 μm) along the longitudinal axis of the tumor and incubated at 70 °C for 2 h to remove the paraffin. The slides were deparaffinized twice with xylene and hydrated using 100, 95, 70, and 60% ethyl alcohol in series. For hematoxylin and eosin (H&E) staining, the samples were washed in running DW and stained with hematoxylin and eosin for 3 min each. Thereafter, the stained slides were fixed and mounted with mounting medium (Muto Pure Chemicals, Tokyo, Japan).

Apoptotic cells were identified using a terminal transferase dUTP nick-end labeling (TUNEL) assay kit (In Situ Cell Death Detection Kit, Roche, Mannheim, Germany) following the manufacturer's protocol. Briefly, the slides were deparaffinized at 70 °C, hydrated, and washed 3 times with PBS-T (0.1% Tween-20 in PBS) for 10 min. The tissue samples were incubated with 1 mg/mL proteinase K (Invitrogen, Carlsbad, CA, USA) in TE buffer at 37 °C for 20 min and washed with PBS-T (0.1% Tween-20 in PBS). The tissues were incubated with 0.1% Triton X-100 at 4 °C for 5 min and treated with a mixture of label solution and enzyme solution (9:1) at 37 °C for 60 min. The slides were counterstained with 4′,6-diamidino-2-phenylindole (DAPI) and mounted with fluorescent mounting solution (DaKo, Glostrup, Denmark). Immunofluorescent images were obtained using an Axio Imager A1 and analyzed with Axiovision Rel. 4.8 software.

For CD31 staining, the slides were hydrated for 5 min and treated with citrate buffer solution at 120–130 °C for 10 min. The slides were washed with PBS and PBS-T (0.05% Tween-20 in PBS) and blocked with 5% bovine serum albumin (BSA; Millipore, Billerica, MA, USA) and 5% horse serum (HS, Gibco, Auckland, New Zealand) in PBS for 90 min at 37 °C. The sections were incubated for 16 h at 4 °C with CD31 antibodies (rabbit anti-mouse CD31; Abcam, Cambridge, UK) diluted in antibody diluent (DaKo, Glostrup, Denmark) (1:200), washed with PBS and PBS-T, and incubated with secondary antibodies (rat anti-mouse Alexa Fluor594; Invitrogen, Carlsbad, CA, USA) for 3 h at room temperature in the dark. The slides were washed with PBS and PBS-T, counterstained with DAPI in DW (1:1000) for 20 min, and mounted with fluorescent mounting solution (DaKo, Glostrup, Denmark).

2.12. Statistical analysis

Cytotoxicity data were obtained from independent experiments in which each treatment condition was tested in quadruplicate. Tumor sizes were evaluated in independent experimental groups with $n = 4$ for each data point. All data are presented as mean ± SD. The results were analyzed by one-way ANOVA with Bonferroni's multiple comparisons test. Statistical analyses were performed with SPSS 12.0 software (IBM Corporation, Armonk, NY, USA).

3. Results

3.1. Preparation of injectable formulations

A concentric nozzle ultrasonic atomizer was used to form Dox-M as reported previously [18–20]. The atomizer produced spherical microcapsules with a smooth surface structure. Fig. 2 shows the prepared Dox-M and the injectable Dox-M formulation. The Dox-M was reddish in color due to the red color of Dox. The yield of the preparation was 74 ± 4%. The mean particle size of the Dox-M was 74 ± 9 μm. The Dox encapsulation efficiency was 54 ± 3%. The microcapsule prepared in this work exhibited relatively high encapsulation efficiency of Dox compared with other research [23].

Aqueous solutions of HP and HC were prepared by dissolving Pluronic® and HC block copolymers in DW and PBS, respectively. Fu-HP and Fu-HC formulations can be prepared easily by simply mixing Fu with HP or HC. Fu-HP and Fu-HC were obtained as a translucent suspension and white suspension, respectively.

To prepare the drug depot for the *in vivo* tumor experiments, Dox-M was readily combined with Fu-HP and Fu-HC to prepare the Dox-M/Fu-HP and Dox-M/Fu-HC formulations. The Dox-M/Fu-HP and Dox-M/Fu-HC formulations were reddish in color. The Dox-M/Fu-HP and Dox-M/Fu-HC formulations were designed to disperse Dox-M inside Fu-HP or Fu-HC; thus, the HP or HC hydrogel acted as an additional outer shell for the Dox-M.

SEM image of *in vivo* Dox-M/Fu-HC depot implant revealed that the Dox-Ms were interspersed in the HC hydrogel, indicating the evidence of the microcapsules inside hydrogel (Fig. 2e and f).

3.2. Characterization of injectable formulations

Dox-M alone, Fu-HP, Fu-HC, Dox-M/Fu-HP, and Dox-M/Fu-HC flowed at room temperature when the vials containing them were tilted. At 37 °C, not all formulations flowed when their vials were tilted. With the exception of the Dox-M, all formulations exhibited distinct solution-to-hydrogel phase transitions at 37 °C.

The thermosensitivity of HP and HC within the formulations was monitored by measuring the solution viscosity as a function of temperature at temperatures ranging from 10 to 60 °C (Fig. 3a). The viscosity of the Dox-M solution was 1 cP at all temperatures. The viscosities of the prepared Fu-HP and Dox-M/Fu-HP formulations at 37 °C were 2.9×10^6 and 2.3×10^6 cP, respectively. Fu-HC and Dox-M/Fu-HC exhibited viscosities of 1.4×10^5 and 3.7×10^4 cP, respectively. These results indicated that the viscosity of Fu-HP was higher than that of Fu-HC at 37 °C. Moreover, viscosity slightly decreased upon the addition of the Dox-Ms.

Although the solutions of Dox-M, Fu-HP, Fu-HC, Dox-M/Fu-HP, and Dox-M/Fu-HC exhibited different viscosities as depots at 37 °C, all formulations formed depots almost immediately after injection into the subcutaneous dorsum of a mouse using a 21-gauge needle (Fig. 2d).

To investigate the maintenance of the depot at body temperature, we measured the viscosities of Fu-HP, Fu-HC, Dox-M/Fu-HP, and Dox-M/Fu-HC, as well as HP alone and HC alone for comparison, at 37 °C for 50 h (Fig. 3b).

At the initial time point (20 min), the viscosities of HP alone, Fu-HP, and Dox-M/Fu-HP were 2.8×10^6, 2.8×10^6, and 1.6×10^6 cP, respectively. The viscosity of the depot slightly decreased on the addition of Fu or Dox-M. The viscosities of HP alone, Fu-HP, and Dox-M/Fu-HP remained approximately constant for 20 h, followed by a gradual decrease to a viscosity of one cP at 50 h.

At 20 min, HC alone, Fu-HC, and Dox-M/Fu-HC exhibited viscosities of 5.4×10^5, 1.0×10^5, and 5.4×10^4 cP, respectively. These results indicated that the viscosity of Fu-HC was lower than that of Fu-HP at 37 °C at the time of the initial formation of the depot. However, the viscosities of HC alone, Fu-HC, and Dox-M/Fu-HC gradually increased up to the 50 h time point, indicating maintenance of the formed depot. The hydrophobic interactions of HP was higher than that of HC at initial time, but the hydrophobic aggregation of HP maintained for shorter residence times than that of HC.

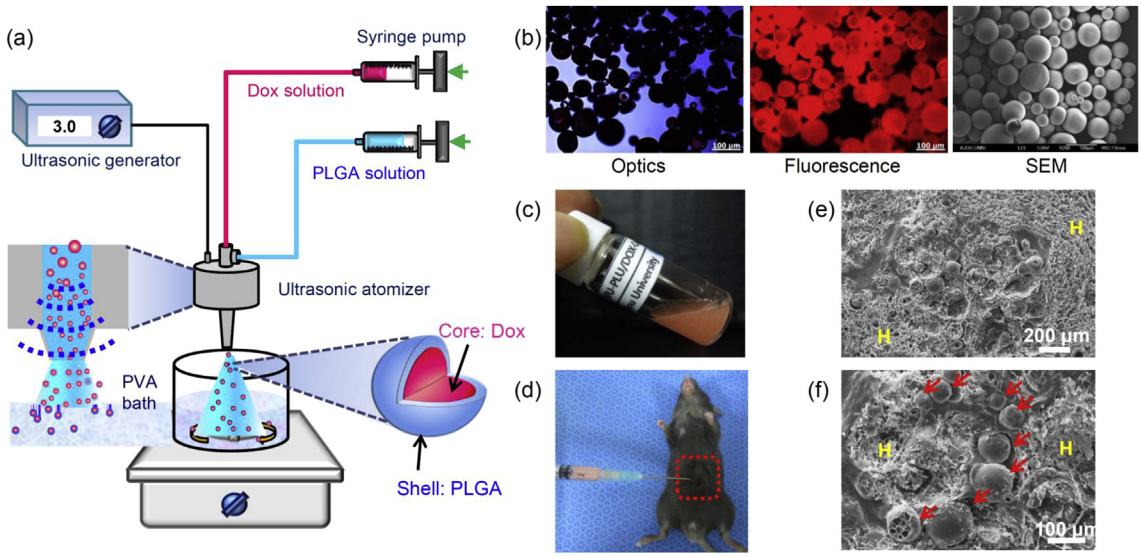

Fig. 2. (a) Schematic representation of the encapsulation method using a mono-axial ultrasonic atomizer; (b) optical microscopy, fluorescence microscopy, and scanning electron microscopy (SEM: 200 × magnification) images of tissue morphology following intratumoral injection of Dox-M; (c) Dox-M/Fu-HC; (d) Dox-M/Fu-HC in mice bearing B16F10 cancer cell xenografts; and (e,f) SEM image of excised Dox-M/Fu-HC depot implants at the time of after 1 day (e) ×200 and (f) ×500 (H indicates the HC hydrogel and arrows indicates Dox-M).

This is owing to that the ability of maintaining the aggregation degree and strength of the hydrophobic segment in HP is remarkably lower than that of HC according to incubation time increased [22].

The gelation and mechanical properties for injectable formulation were further analyzed by rheology with change in frequency from 0.1 to 10 Hz at room temperature and 37 °C. In the strain sweep test, the limiting strain amplitudes of HP and HC were 1.6 and 4.0%, respectively, indicating the stability of HC compared to HP (Supplementary Fig. S1). The storage modulus (G') value of HP and HC increased with changing of temperature from room temperature to 37 °C (Fig. 3c). HP and HC also exhibited greater viscosity at 37 °C than those at room temperature (Fig. 3d). In addition, HP and HC showed the gel-like features in phase angle (tan delta) according to increasing temperature from room temperature to 37 °C (Fig. 3d). These results indicated a typical phase transition to elastic gel-like from solution as function of temperature and a characteristic feature of HP and HC as injectable formulation.

Fig. 3f showed the viscosities for Fu-HP, Fu-HC, Dox-M/Fu-HP and Dox-M/Fu-HC after addition of Fu and Dox. There was little or no change in viscosities of HP and HC even after Fu and Dox, indicating the stability of HP and HC. The G' value of Fu-HP and Dox-M/Fu-HP exhibited a higher than those of Fu-HC and Dox-M/Fu-HC at 37 °C.

Taken altogether, the Dox-M/Fu-HP and Dox-M/Fu-HC showed a characteristic feature as injectable formulation according to changing of temperature from room temperature to 37 °C.

Fig. 4A shows changes in Dox-M alone, Dox-M/Fu-HP, and Dox-M/Fu-HC occurring owing to incubation at 37 °C. After incubation at 37 °C for 2 days, the depots formed from the Fu-HP and Dox-M/Fu-HP formulations became liquid. In contrast, the Fu-HC and Dox-M/Fu-HC depots maintained a gelatinous form for up to 3 weeks at 37 °C, indicating that depots formed from Fu-HC and Dox-M/Fu-HC maintained their structural gelatinous integrity.

To examine the *in vivo* persistence and biodegradability of HP and HC, the injected HP and HC implants were individually recovered. However, the HP implant could not be recovered, because HP completely disappeared 2–3 days after the injection, likely owing to disentanglement of HP rather than biodegradation.

The HC implant was maintained as a depot for 18 days and showed a slight decrease in size at 18 days after injection, reaching a final volume of 83% of its original volume (Supplementary Fig. S2). These results indicated that HC could act as a persistent drug depot over a defined experimental period. The ^{1}H NMR spectra of HC showed characteristic peaks assignable to a degraded oligomer, lactic acid, 6-hydroxylhexanoic acid, and the parent HC compound after *in vivo* implantation (Supplementary Fig. S2), indicating that HC can be degraded *in vivo* after a defined experimental period.

3.3. In vitro Dox and Fu release

The *in vitro* Dox and Fu release behavior from Dox-M alone, Fu-HP, Fu-HC, Dox-M/Fu-HP, and Dox-M/Fu-HC was examined at 37 °C for 34 days (Fig. 4B, Table 1 and Supplementary Fig. S3). For Dox-M/Fu-HP, Fu release was 20% at 12 h, 75% at 1 day, and almost 92% at 2 days, followed by no additional release due to disentanglement of the HP depot at 2 days (Fig. 4a). As shown in Fig. 4b, Fu release from Dox-M/Fu-HP showed a C_{max} of 43.7 μg at a T_{max} of 24 h. Meanwhile, Fu release from Dox-M/Fu-HC was 19% at 12 h, 37% at 1 day, and 58% at 2 days, followed by a slower increase in the amount released, with 80% released after 34 days. Fu release from Dox-M/Fu-HC showed a C_{max} of 30.3 μg at a T_{max} of 34 h. Fu-HP showed no remained Fu inside HP hydrogel, but Fu-HC exhibited the remained Fu amount of 7% inside the HC hydrogel, indicating the sustain release of Fu from HC drug depot (Supplementary Fig. S4). The amount of Fu released from Fu-HC was only half of that released from Fu-HP, due to maintenance of structural gelatinous integrity by HC.

For Dox-M alone (Fig. 4c–d), the initial burst release (percentage released in the first day) was 42%. The Dox release was biphasic, with 46% released at 2 days, followed by a plateau for 13 days and a slower increase in release, with 72% released during 34 days. Dox release from Dox-M alone showed a C_{max} of 65.5 μg at a T_{max} of 1 h.

Dox release from Dox-M/Fu-HP was 23% at 1 day and 32% at 2 days. Dox release from Dox-M/Fu-HP showed a C_{max} of 16.6 μg at a T_{max} of 60 h, probably due to retardation of Dox release by the HP depot, which kept viscosity at day 2, acting as an additional outer

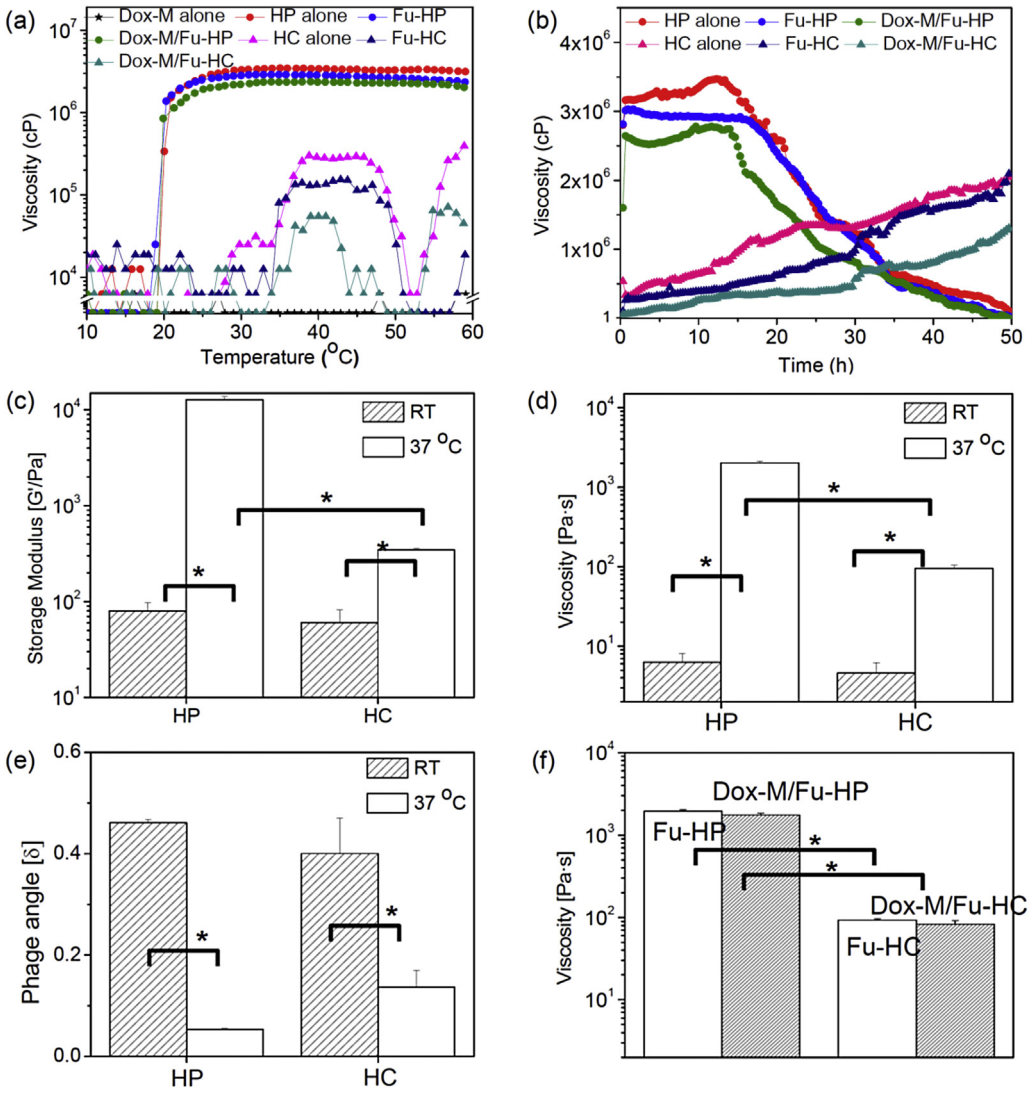

Fig. 3. (a and b) Viscometer measurement; (a) viscosity versus temperature variation and (b) viscosity versus incubation time at 37 °C for Dox-M alone, HP, HC, Fu-HP, Fu-HC, Dox-M/Fu-HP, and Dox-M/Fu-HC. (c–f) Rheology measurement at room temperature and 37 °C; (c) storage modulus, (d) viscosity and (e) phase angle for HP, HC, and (f) viscosity at 37 °C for Fu-HP, Fu-HC, Dox-M/Fu-HP and Dox-M/Fu-HC. (*$p < 0.001$).

shell for the Dox-Ms. After 3–4 days, Dox release from Dox-M/Fu-HP showed a pattern similar to that of Dox alone, followed by a slower increase in release, with 68% released after 34 days, probably due to dissipation of the HP depot.

The Dox-M/Fu-HP formulation exhibited high viscosity after short periods at body temperature (as shown in Fig. 3a), but dissipation of HP was apparent after only 2 days (as shown in Figs. 3b and 4A). The high viscosity of the Dox-M/Fu-HP formulation resulted in significant suppression of the initial burst release of Dox, but the release rate increased after a short time and Dox-M/Fu-HP showed Dox release similar in duration to that of Dox-M.

Dox release from Dox-M/Fu-HC was 20, 25, and 52% at 1, 2, and 34 days, respectively. Dox release from Dox-M/Fu-HC showed a C_{max} of 14.3 μg at a T_{max} of 4 h. The Dox-M/Fu-HC formulation showed medium gel strength after short periods at body temperature (as shown in Fig. 3a), but maintained its depot structure after approximately 3 weeks (as shown in Fig. 4), resulting in a sustained-release profile through moderate suppression of the initial burst release and maintenance of Dox release for a duration of 34 days.

The T_{max} and C_{max} values for Dox release from Dox-M/Fu-HP and Dox-M/Fu-HC were significantly higher and lower, respectively, than those of the Dox-M alone. After 34 days, the amounts of remaining Dox in the Dox alone, Dox-M/Fu-HP, and Dox-M/Fu-HC depots decreased to approximately 18, 19, and 31%, respectively (Supplementary Fig. S4). The decreases in the rate and amount of Dox release were due retardation of Dox release by the HC hydrogel, which acted as an additional outer shell for the Dox-M. These results indicated that hydrogels with different gel persistence can be utilized to control the release behavior of Fu from Fu-H and of Dox from Dox-M. This indicated that *in vitro* release was less than 100% of Fu and Dox due to the remained drug in the microcapsules and hydrogels.

3.4. Anti-proliferative effects of the formulations

Since melanoma is one of the most dangerous types of skin cancer, we chose B16F10 cancer cells to establish intratumoral animal model through subcutaneous inoculation. Firstly, the anti-proliferative activities of PBS, free Fu, free Dox, free Dox/Fu, Dox-

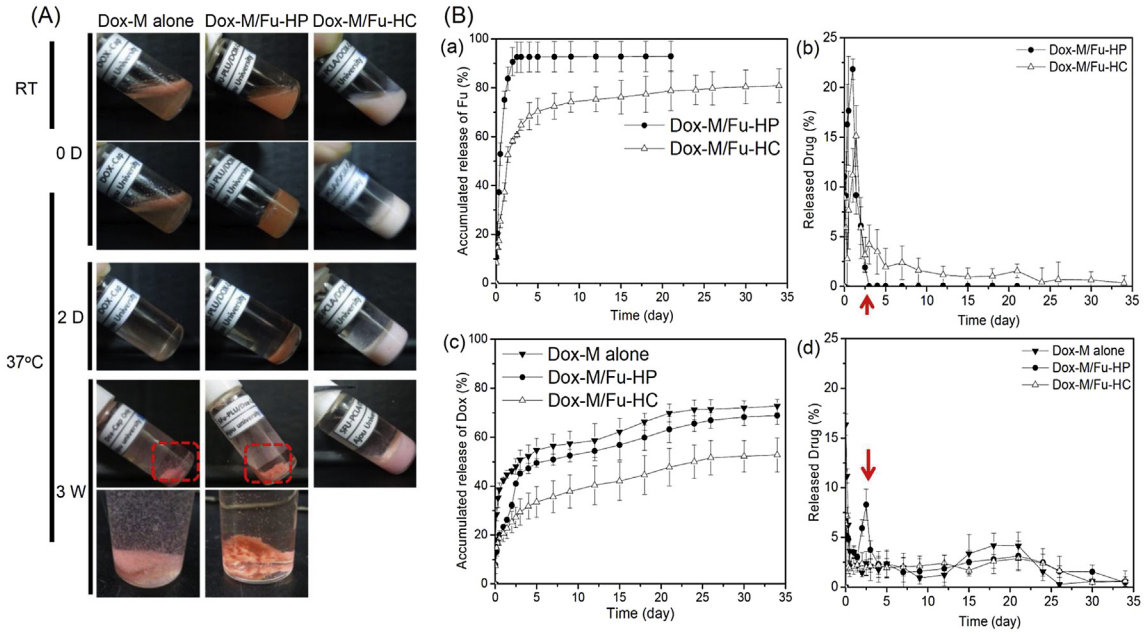

Fig. 4. (A) Images of the formulations of Dox-M alone, Dox-M/Fu-HP, and Dox-M/Fu-HC at room temperature and 37 °C for 0–3 weeks. (B) Accumulated release of (a, b) Fu and (c, d) Dox after 34 days and the released amount of (b) Fu and (d) Dox at each time point from Dox-M/Fu-HP, Dox-M/Fu-HC, Dox-M alone, Dox-M/Fu-HP, and Dox-M/Fu-HC for 34 days.

Table 1
T_{max} and C_{max} of the released Fu and Dox amount at corresponding time (determined from graph in Fig. 4b, d).

	Fu			Dox	
	T_{max} (h)	C_{max} (μg)		T_{max} (h)	C_{max} (μg)
Dox-M/Fu-HP	24	43.7 μg	Dox-M alone	1	65.5
Dox-M/Fu-HC	34	30.3 μg	Dox-M/Fu-HP	60	16.6
			Dox-M/Fu-HC	4	14.3

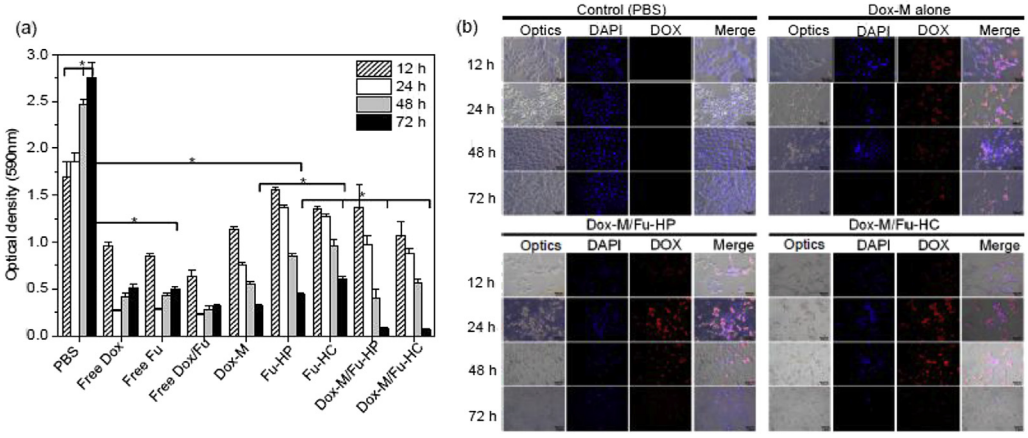

Fig. 5. (a) Viability of B16F10 cancer cells exposed to the test formulations as measured by the MTT assay. Cells grown on a culture plate were used as a control group. Statistical analyses were performed using one-way ANOVA with Bonferroni's multiple comparison test (*$p < 0.001$). (b) Optical and fluorescent images showing the morphology of B16F10 cells treated with PBS, Dox-M alone, Dox-M/Fu-HP, and Dox-M/Fu-HC after 12, 24, 48, and 72 h. The scale bars represent 50 μm (400 × magnification).

M alone, Fu-HP e, Fu-HC, Dox-M/Fu-HP, and Dox-M/Fu-HC were assessed in B16F10 cancer cells cultured for 72 h (Fig. 5). Cells treated with PBS showed an increase in the cell population as a function of culture time.

After the addition of free Fu, free Dox, and free Dox/Fu, cell viability decreased to approximately 40–50% at 12 h and 11–14% at 24 h, in comparison with that of the cells treated with PBS. Thereafter, cell viability was below 15% in comparison with that of the cells treated with PBS, despite replacement of the medium containing free Fu, free Dox, or free Dox/Fu with fresh culture medium at 12 h. These results indicate that free Fu, free Dox, and free Dox/Fu produced anti-proliferative effects on B16F10 cancer cells. The free Dox/Fu combination inhibited cell proliferation more effectively than free Fu or free Dox alone ($p < 0.001$).

The population of cells exposed to Dox-M alone, Fu-HP, Fu-HC, Dox-M/Fu-HP, and Dox-M/Fu-HC gradually decreased as a function of culture time, indicating that the depot formed from the formulation produced sustained release of Dox and Fu.

After the addition of Dox-M alone, cell viability decreased to approximately 65%, 40%, 20% and less than 10% of that of the control

cells at 12, 24, 48, and 72 h, respectively, indicating that the Dox released from the Dox-M led to persistent cell death. Following the addition of Fu-HP and Fu-HC, cell viability was slightly higher than that observed following the addition of Dox-M alone.

The populations of cells exposed to Dox-M/Fu-HP and Dox-M/Fu-HC were greater than the populations of those exposed to free Fu, free Dox, and free Dox/Fu, but cell counts gradually decreased as a function of culture time. The cell populations were nearly abolished at 48 and 72 h, indicating that the released Dox and Fu nearly completely inhibited cell viability. These results indicated that the released Fu and Dox produced nearly complete anti-proliferative effects.

Optical and fluorescent images of B16F10 cancer cells were obtained after exposure to Dox-M alone, Fu-HP, Fu-HC, Dox-M/Fu-HP, and Dox-M/Fu-HC (Fig. 5b and Supplementary Fig. S5). Blue fluorescence was indicative of Hoechst-stained nuclei. Dox showed as red fluorescence, while pink fluorescence was due to the overlay of the blue and red fluorescent images.

The control cells showed an increase in the cell population in the optical and blue fluorescent images at 72 h. The cells treated with Dox-M alone showed decreased blue fluorescence as a function of culture time. Pink fluorescence was observed in the nuclei of the B16F10 cancer cells in the merged images. Blue, red, and pink fluorescence further decreased with incubation time. These results imply that the Dox released from the Dox-M penetrated B16F10 cancer cells and induced cell death.

Distinct pink fluorescence was observed in the cells treated with Dox-M/Fu-HP and Dox-M/Fu-HC. Pink fluorescence in the cytoplasm gradually decreased with incubation time and disappeared at 72 h, suggesting that extended exposure time enhanced the effects of the released drugs and thus induced nearly complete the cell death.

3.5. Antitumor efficacy of the combination therapy

Saline, Dox-M alone, Fu-HP, Fu-HC, Dox-M/Fu-HP, and Dox-M/Fu-HC were intratumorally injected into the tumors. The change in tumor volume from the initial volume was monitored for 18 days after intratumoral injection (Fig. 6 and Supplementary Fig. S6). In mice injected with the saline solution, tumor size gradually increased as a function of time, reaching a size approximately 60 times that of the original tumor after 18 days. In contrast, Dox-M alone suppressed tumor growth, restricting the total increase in tumor volume to approximately 20 times the original tumor size.

Intratumoral injection of Fu-HC, Dox-M/Fu-HP and Dox-M/Fu-HC reduced the overall tumor growth rate in comparison with saline, Fu-HP or Dox-M alone. Suppression of growth by Dox-M/Fu-HP showed a slope over 4–5 days similar to that of Dox-M/Fu-HC, after which there was a gradual increase in the slope. Strikingly, almost no tumor growth was observed in animals injected with Dox-M/Fu-HC for 10 days, after which there was a slight increase in tumor volume in comparison with that of the animals injected with Dox-M/Fu-HP. There was no significant change in the body weight of the mice following treatment (Supplementary Fig. S7).

The tumor volume doubling times (DTs) and tumor growth rates are summarized in Table 2. Injections of saline resulted in a very short DT of about 2.8 days. Injection of Dox-M alone and Fu-HP extended the DT to about 5 days and 3 days, respectively. In addition, Dox-M alone and Fu-HP reduced the rate of tumor growth to about 102 mm^3 per day and reduced 350 mm^3 per day, respectively, whereas that of the saline group was about 440 mm^3 per day. Dox-M/Fu-HP injection significantly extended the DT (7.6 days) and decreased the rate of tumor growth (to 45 mm^3 per day) in comparison with the saline group.

Fu-HC extended DT to about 6 days and reduced 45 mm^3 per day, indicating that Fu-HC produced more significant inhibitory effects against tumor growth than the saline group. In addition, in mice that received an intratumoral injection of Dox-M/Fu-HC, the tumor volume DT remarkably increased to 11 days, while the tumor growth rate decreased to 21 mm^3 per day. Dox-M/Fu-HC produced more significant inhibitory effects against tumor growth than Dox-M/Fu-HP or Dox-M alone.

3.6. Biodistribution of Dox and Fu

The biodistribution of Dox in tissues was observed by fluorescence microscopy 1, 6, 12, and 18 days after injection (Supplementary Fig. S8). A considerable amount of Dox was observed in fluorescent images of the tumor on days 1, 6, 12, and 18 after injection of Dox-M alone, Dox-M/Fu-HP, and Dox-M/Fu-HC. However, the intestines, stomach, lung, kidney, liver, spleen, and heart showed very weak Dox fluorescence (red) following injection of Dox-M alone, Dox-M/Fu-HP, and Dox-M/Fu-HC.

The amounts of Fu and Dox in tumors and various organs were quantified (Fig. 7). One day after injection of Dox-M alone, the tumor contained approximately 30% of the administered Dox, but this quantity decreased to approximately 20% and 7% after 6 and 12

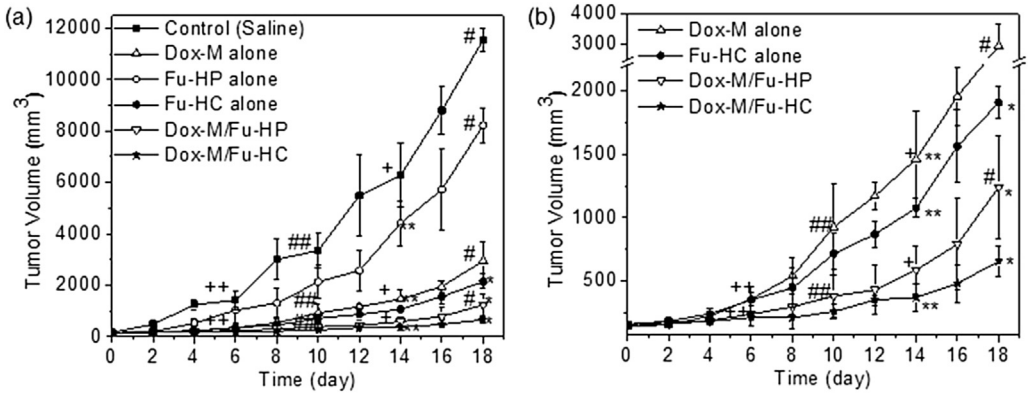

Fig. 6. Inhibitory effects of (a) full tumor volume and (b) enlarged tumor volume for saline, Dox-M alone, Fu-HP, Fu-HC, Dox-M/Fu-HP, and Dox-M/Fu-HC. Each solution was injected into xenograft-bearing mice after the initial tumor had reached a volume of 150–200 mm^3. Statistical analyses were performed using one-way ANOVA with Bonferroni's multiple comparison test ($p < 0.001$ versus the saline-injected group at 6 [++], 10 [##], 14 [+], and 18 [#] days; $p < 0.01$ versus the Dox-M/Fu–HC–injected group at 14 [**] and 18 [++] days).

Table 2
Tumor volume doubling times and tumor growth rate after intratumoral injection.

	Saline	Dox-M alone	Fu-HP	Fu-HC	Dox-M/Fu-HP	Dox-M/Fu-HC
Tumor volume doubling time (days)	2.8 ± 1.0	5.2 ± 0.1[a]	3.0 ± 0.2[b]	6.3 ± 0.1[a]	7.6 ± 2.1[a,b]	11.2 ± 2.4[a,b]
Tumor growth rate (mm^3/day)	438 ± 90	101.9 ± 22.1[a]	348 ± 198[b]	97.1 ± 6.9[a]	45.1 ± 13.9[a,b]	21.3 ± 5.6[a,b,c]

Statistical analyses were performed using one-way ANOVA with Bonferroni's post-hoc test. Statistical analyses were performed with SPSS 12.0 software (SPSS Inc, IL, USA).
[a] $p < 0.01$, versus control at the same time-point.
[b] $p < 0.01$, versus Dox-M only at the same time-point.
[c] $p < 0.05$, versus Dox-M/Fu-HP at the same time-point.

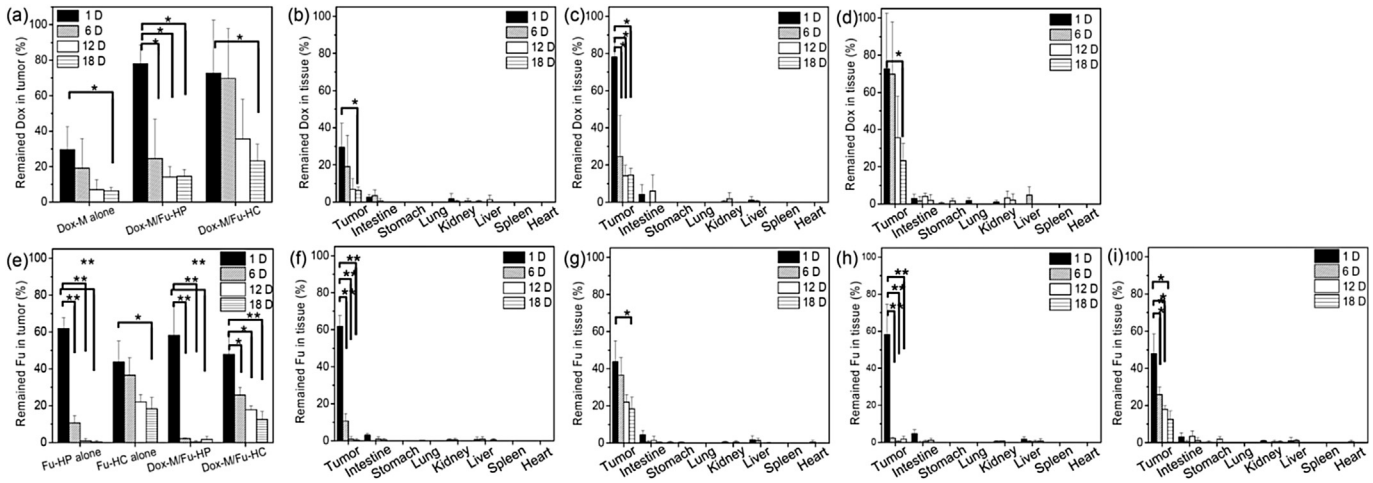

Fig. 7. Distribution of (a) Dox in tumors after intratumoral injection of Dox-M alone, Dox-M/Fu-HP, and Dox-M/Fu-HC, as well as Dox distribution in all organs after intratumoral injection of (b) Dox-M alone, (c) Dox-M/Fu-HP, and (d) Dox-M/Fu-HC (*$p < 0.05$). Distribution of (e) Fu in tumors after intratumoral injection of Dox-M alone, Fu-HP alone, Fu-HC alone, Dox-M/Fu-HP, and Dox-M/Fu-HC, as well as in all organs after intratumoral injection of (f) Fu-HP, (g) Fu-HC, (h) Dox-M/Fu-HP and (i) Dox-M/Fu-HC (*$p < 0.05$, **$p < 0.001$).

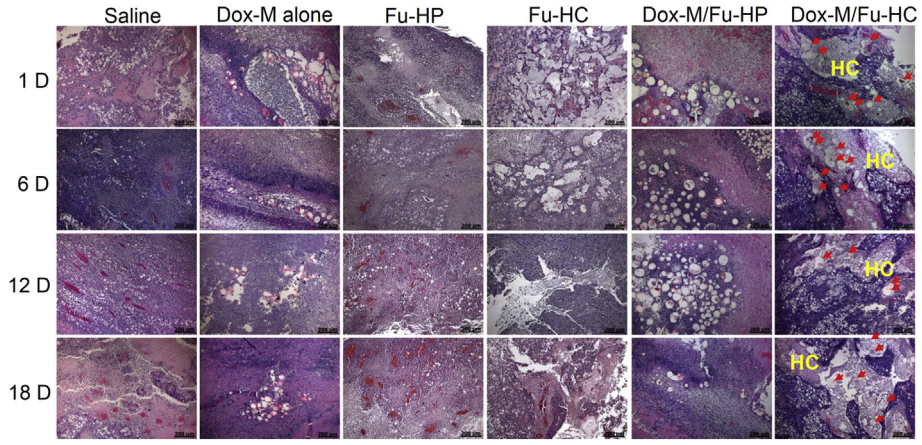

Fig. 8. H&E-stained histological sections of tumors on days 1, 6, 12, and 18 after intratumoral injection of xenograft-bearing mice with saline, Dox-M alone, Fu-HP, Fu-HC, Dox-M/Fu-HP, and Dox-M/Fu-HC. The arrows indicate microcapsules with hydrogel (scale bar = 200 μm).

days, respectively. For the injection of Fu-HP, the tumor contained Fu of 50% at one day and 1% even at 12 days, while Fu-HC remained 40–20% of the administered Fu, indicating the sustained release of Fu from HC.

One day following injection of Dox-M/Fu-HP, the tumor contained approximately 15% of the administered Fu and 80% of the administered Dox; however, only 3% of Fu and 25% of Dox remained in the tumor after 6 days. This rapid decrease in drug concentrations in the tumor was probably due to the disentanglement of the HP hydrogel, which acted as an additional outer shell.

One day following injection of Dox-M/Fu-HC, the tumor contained approximately 50% of the administered Fu and 70% of the administered Dox. Six days following injection of Dox-M/Fu-HC, 25% of Fu and 68% of Dox remained in the tumor. Eighteen days following injection of Dox-M/Fu-HC, 13% of Fu and 22% of Dox remained in the tumor, due to the gelatinous structural integrity contributed by HC acting as an additional outer shell.

These results indicate that direct intratumoral injection of Dox-M alone, Dox-M/Fu-HP, and Dox-M/Fu-HC significantly enhances the distribution of Fu and Dox to the tumor. In addition, Fu and Dox were sustainably released from HC and microcapsules, respectively. Furthermore, Dox release was retarded by the HC hydrogel, which

acted as an additional outer shell for the Dox-M.

3.7. Histology studies

The tumors treated with saline, Dox-M alone, Fu-HP, Fu-HC, Dox-M/Fu-HP, and Dox-M/Fu-HC were stained for histological analysis. Fig. 8 shows H&E-stained histological sections of formulation-treated tumors on days 1, 6, 12, and 18. The treated tumors were viable. The number of blood vessels was observed 1 day after intratumoral injection of the formulations. The number of blood vessels in the tumors treated with saline was unchanged, while the tumors treated with Dox-M alone, Fu-HC, Dox-M/Fu-HP, and Dox-M/Fu-HC showed decreased numbers of blood vessels as the implantation time increased. Microcapsules were observed at the injected tumor for the full experimental period of 18 days.

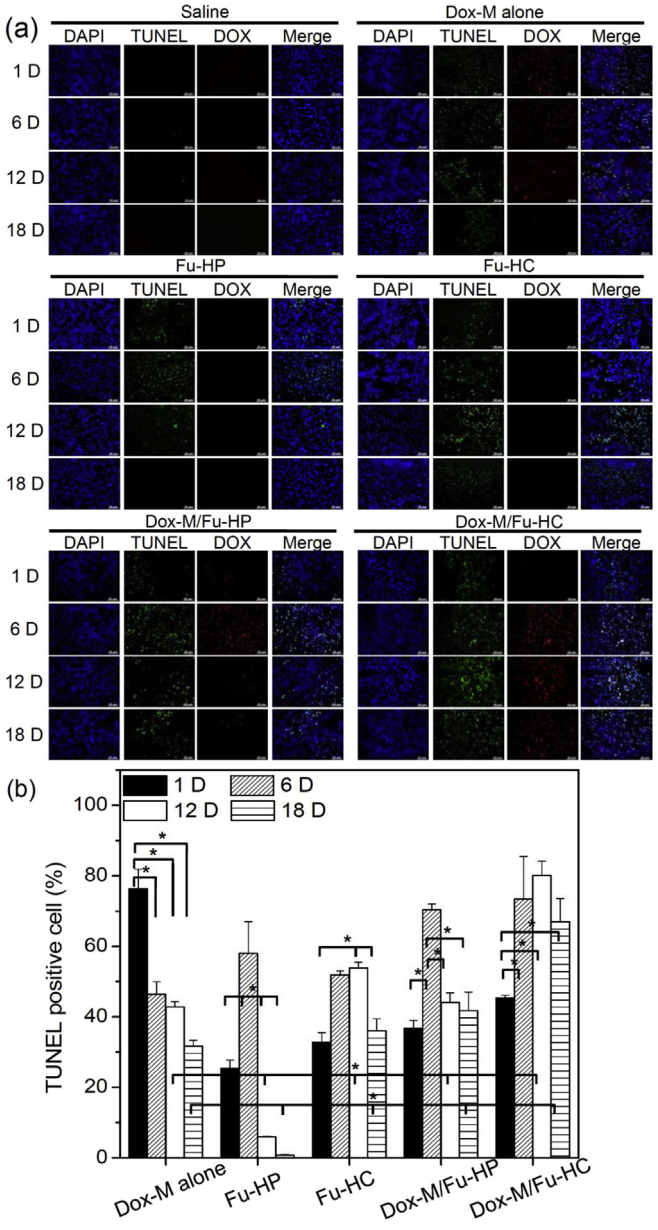

Fig. 9. (a) DAPI staining (blue, nuclei), TUNEL staining (green, apoptotic cells), Dox (red), and merged images of tumors on days 1, 6, 12, and 18 after intratumoral injection of xenograft-bearing mice with saline, Dox-M alone, Fu-HP, Fu-HC, Dox-M/Fu-HP, and Dox-M/Fu-HC (scale bar = 50 μm). (b) Number of TUNEL-positive cells in images of cells from tumors injected with Dox-M alone, Fu-HP, Fu-HC, Dox-M/Fu-HP, and Dox-M/Fu-HC (*$p < 0.01$). (For interpretation of the references to colour in this figure legend, the reader is referred to the web version of this article.)

Fig. 9a presents images showing DAPI staining (nuclei), TUNEL staining (apoptosis), red fluorescence (Dox), and a merge of the 3 images for the tumors treated with saline, Dox-M alone, Fu-HP, Fu-HC, Dox-M/Fu-HP, and Dox-M/Fu-HC after 1, 6, 12, and 18 days (Supplementary Fig. S9).

Bright blue fluorescence attributable to DAPI staining of the nuclei of live cells was evident in the formulation-treated tumors. The tumors treated with Dox-M alone, Dox-M/Fu-HP, and Dox-M/Fu-HC showed red fluorescence owing to the release of Dox from Dox-M, but no red fluorescence was observed in the Fu-HP, Fu-HC and saline-treated tumors. The green fluorescence of TUNEL staining corresponding to apoptotic cells was absent in the tumors treated with saline. In contrast, a high degree of green fluorescence from TUNEL staining was detected in tumors injected with Dox-M alone, Fu-HP, Fu-HC, Dox-M/Fu-HP, and Dox-M/Fu-HC, indicating large numbers of apoptotic cells.

The merge of the 3 images showed bright white areas, indicating areas of overlap that could provide distinct evidence of tumor cell apoptosis induced by release of Dox from Dox-M. The observed necrotic effects were congruent with the observed suppression of tumor growth.

TUNEL-positive cells were counted and normalized to the total stained tissue area in order to determine the extent of apoptosis (Fig. 9b). The percentage of apoptotic cells (TUNEL-positive cells) in the group treated with Dox-M alone was 78% at 1 day and decreased to about 30–40% as the implantation time increased, indicating that there was a high rate of apoptosis due to an initial burst of Dox from Dox-M alone at 1 day, which decreased to the decreasing amount of Dox released from the Dox-M as the implantation time increased.

In the case of intratumoral injections of Fu-HP alone, the apoptosis was 25% at 1 day due to the little release of Fu from relatively strong HP hydrogel, increased to 60% at 6 days by the large amount of Fu release due to the short residence times of HP hydrogel, and then decreased to 5% and 1% after 12 and 18 days respectively. The rate of apoptosis for Dox-M/Fu-HP increased to 70% due to the Fu released from Fu-HP, as well as Dox released from Dox-M, and then decreased to 44% and 42% after 12 and 18 days respectively.

The apoptosis of Fu-HC was 33% at 1 day due to the relatively weak HC hydrogel, increased to ~55% at 6–12 days and then decreased to 35%, indicating the sustained release of Fu from Fu-HC. Dox-M/Fu-HC also produced a slightly higher rate of apoptosis in comparison with that produced by Dox-M/Fu-HP at 1 day due to lower viscosity, as explained previously. However, the rate of apoptosis was maintained at 70–80% as the implantation time increased. This finding indicated that Fu and Dox remained in the HC hydrogel due to the HC hydrogel acting as an additional outer shell for the Dox-M.

To compare the number of blood vessels in tumors treated with the formulations, tumor tissue samples were stained with CD31 at 1, 6, 12, and 18 days after intratumoral injection of saline, Dox-M alone, Fu-HP, Fu-HC, Dox-M/Fu-HP, and Dox-M/Fu-HC (Fig. 10 and Supplementary Fig. S10). The tumors treated with saline showed CD31-positive red staining due to blood vessels, which increased as the implantation time increased. The tumors treated with Dox-M alone, Fu-HP alone, Fu-HC alone, Dox-M/Fu-HP, and Dox-M/Fu-HC showed increased CD31 staining as the implantation time increased.

The CD31-positive red images were normalized to the total stained DAPI area in order to determine the extent of blood vessel formation (Fig. 10b). One, 6, 12, and 18 days following saline

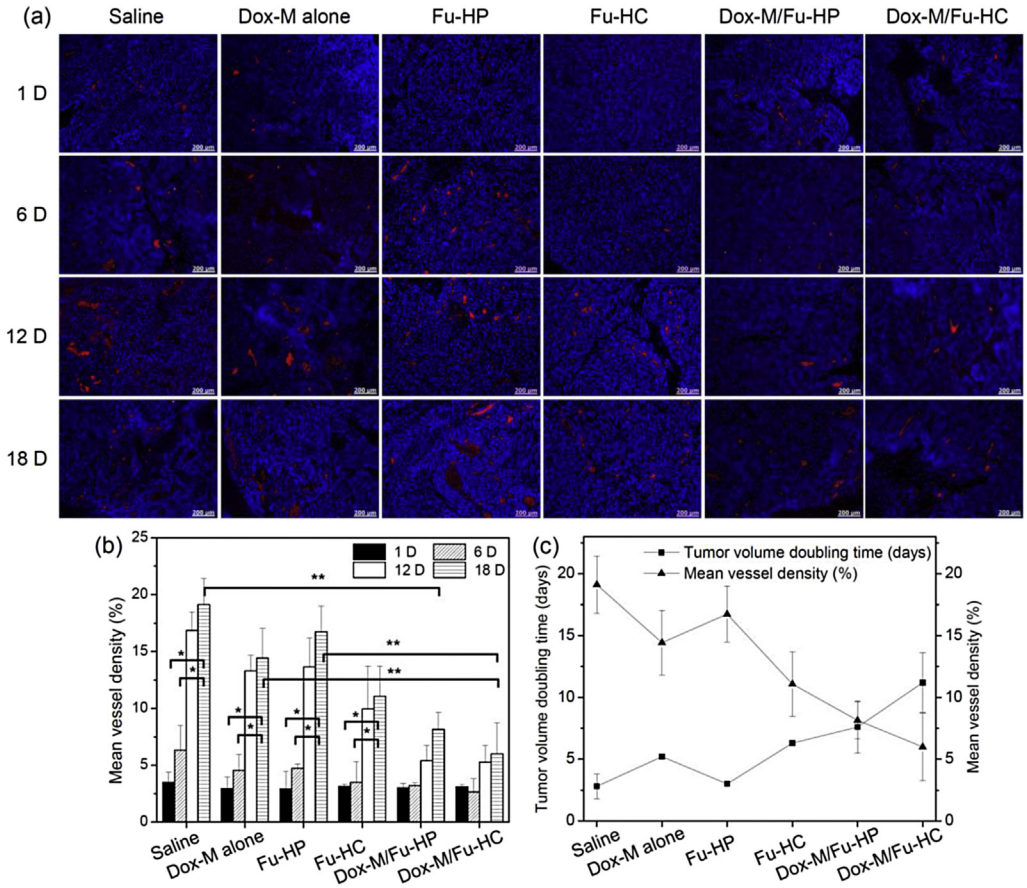

Fig. 10. (a) DAPI staining (blue, nuclei), CD31 staining (red, tumor vasculature), and merged images of tumors on days 1, 6, 12, and 18 after intratumoral injection of xenograft-bearing mice with saline, Dox-M alone, Fu-HP, Fu-HC, Dox-M/Fu-HP, and Dox-M/Fu-HC (scale bar = 200 μm). (b) Mean vessel densities in images of tumors injected with saline, Dox-M alone, Fu-HP alone, Fu-HC alone, Dox-M/Fu-HP, and Dox-M/Fu-HC. All analyses were performed using 3 random fields for each slide ($^{*}p < 0.01$, $^{**}p < 0.05$). (c) Tumor volume doubling time versus mean vessel density for tumors injected with saline, Dox-M alone, Fu-HP, Fu-HC, Dox-M/Fu-HP, and Dox-M/Fu-HC. (For interpretation of the references to colour in this figure legend, the reader is referred to the web version of this article.)

administration, the extent of blood vessel formation was gradually increased to 3.4%, 6.3%, 16.8%, and 19.1% ($^{*}p < 0.01$), respectively. One, 6, 12, and 18 days following administration of Dox-M alone, the extent of blood vessel formation increased to 3.3%, 4.5%, 13.3%, and 14.4%, respectively, probably owing to initial suppression of blood vessel formation by the initial burst of Dox release, followed by blood vessel formation slower than that of the saline-treated tumors due to slow release of Dox from Dox-M.

For Fu-HP, the extent of blood vessel formation increased to 2.9%, 4.7%, 13.6%, and 16.7%, respectively. Meanwhile, the Fu–HC–treated tumors showed lower extent of blood vessel formation (3.1%, 3.5%, 10.0%, and 11.1% at corresponding time) than those of Fu-HP. Following intratumoral injections of Dox-M/Fu-HP and Dox-M/Fu-HC, the extent of blood vessel formation reduced in comparison with that of tumors treated with Dox only. After 1, 6, 12, and 18 days, the extent of blood vessel formation in the Dox-M/Fu-HP-treated tumors was gradually increased to 3.0%, 3.2%, 5.4%, and 8.1%, respectively ($^{**}p < 0.05$). After 1, 6, 12, and 18 days, the extent of blood vessel formation in the Dox-M/Fu–HC–treated tumors was gradually increased to 3.1%, 2.7%, 5.3%, and 6.0%, respectively ($^{**}p < 0.05$). These results indicated that intratumoral injection of Dox-M/Fu-HP and Dox-M/Fu-HC significantly suppressed the formation of blood vessels extending into the tumor, restricting tumor growth. Therefore, the tumor volume DT was correlated with blood vessel density (Fig. 10c). This finding indicated that sustained release of Fu from HP or HC and Dox from Dox-M suppressed blood vessel formation in the treated tumors and increased tumor volume DTs.

4. Discussion

Because parenteral Dox and Fu have short half-lives in blood [8–10], frequent administration of these drugs is required. Various approaches have been utilized to maintain *in vivo* therapeutic concentrations of Dox and Fu within target tumors and thus avoid systemic toxicity. Several investigators, including our group, have examined injectable drug depot systems [15–17,24]. Hydrogels and microcapsules loaded with Dox or Fu have recently emerged as an attractive drug depots and promising clinical modalities. Thus, intratumoral administration of injectable drug depots of Dox and/or Fu has been adopted in the current work.

In the present study, injectable formulations of Dox and Fu were easily prepared by mixing Dox-M with Fu-H. The prepared Dox-M/Fu-HP and Dox-M/Fu-HC formulations flowed at room temperature, indicating injectability, and formed a structural gelatinous hydrogel *in vitro* and *in vivo* at 37 °C, indicating the formation of depots. The solution-to-hydrogel phase transitions were due to the thermosensitivity of HP and HC [22]. HP exhibited quick phase transitions, but the formed hydrogel disappeared after 2 days due to disentanglement of HP *in vitro* and *in vivo*, instead of biodegradation. In contrast, HC persisted for a long period in the injected tissue and showed slow biodegradation *in vivo*.

Intravenously injected free Dox and Fu are metabolized and show weak stability *in vivo* [8–10], limiting their clinical use. However, the Dox-M/Fu-HP and Dox-M/Fu-HC formulation depots utilized in this work showed sustained release of Fu from the hydrogel and of Dox from the microcapsules, which was extended by the outer hydrogel shell. The formulations of Dox-M alone, Fu-HP, Fu-HC, Dox-M/Fu-HP, and Dox-M/Fu-HC gradually decreased cell populations *in vitro*. Specifically, Dox-M/Fu-HP and Dox-M/Fu-HC led to almost complete cell death as a function of culture time, indicating that the formulations reported herein worked well as drug depots.

For the *in vivo* tumor suppression experiment, Dox-M alone, Fu-HP, Fu-HC, Dox-M/Fu-HP, and Dox-M/Fu-HC were easily injected into the centers of tumors in mice using a 21-gauge needle. Dox-M alone, Fu-HC, Dox-M/Fu-HP, and Dox-M/Fu-HC formed drug depots rather than spreading or dissipating at the tumor site. Fu-HP completely disappeared 2–3 days after the injection due to disentanglement of HP. The Dox-M/Fu-HC formulation inhibited tumor growth more effectively than Dox-M alone, Fu-HP, Fu-HC, or Dox-M/Fu-HP. This indicated that combinational intratumoral injection exhibited synergistic anti-tumor activity.

The *in vivo* Dox and Fu biodistribution data showed that high Dox and Fu concentrations were maintained in the target tumor only for 18 days, without distribution of the drugs to normal tissues. These findings were probably due to sustained drug release via the confinement of Dox and Fu within the hydrogel and microcapsules, respectively. In addition, these results indicate that Dox and Fu at concentrations below their respective toxic plasma concentrations should not cause significant systemic toxicity in cancer patients. Based on the results of the intratumoral injection experiments, it was reasonable to conclude that a single injection of the Dox-M/Fu-HP and Dox-M/Fu-HC combination formulations could synergistically inhibit tumor growth *in vivo*. Because the hydrogel formed a drug depot through gelation at body temperature after the injection, hydrogel persistence times can be used to fine-tune tumor inhibition.

Collectively, these results indicate that intratumoral injection of Dox-M/Fu-HP and Dox-M/Fu-HC might allow Dox and Fu to specifically accumulate in the tumor and maintain long-lasting tumor suppression with little toxicity to other organs.

5. Conclusion

This work showed that Dox-M/Fu-HP and Dox-M/Fu-HC could act as an anticancer drug depot capable of providing sustained release of Fu and/or retarding the release of Dox after intratumoral injection. In addition, in comparison with a single injection of Dox-M, intratumoral injections of Dox-M/Fu-HP or Dox-M/Fu-HC produced significantly longer local Fu and Dox retention in tumors. Although there is still remaining for the safety issue in experimental setting, we believe that these results can provide a rationale for tumor treatment toward patient with breast cancer to go clinical translation through combination therapy.

Acknowledgments

This study was supported by a grant from a Basic Science Research Program (2013R1A2A2A04014200 and 2014M3A9E5073700) and Priority Research Centers Program (2010-0028294) through the National Research Foundation of Korea (NRF) funded by the Ministry of Education.

Appendix A. Supplementary data

Supplementary data related to this article can be found at http://dx.doi.org/10.1016/j.biomaterials.2016.02.001.

Author contributions

D.Y.K., D.Y.K, J.H.P., S.H.P., and H.J.O. designed and carried out experiments. D.Y.K., D.Y.K., and J.S.K carried out cell experiments. D.Y.K., J.H.P., and S.H.P. carried out animal experiments. D.Y.K., S.H.P., H.J.O., B.H.M., and K.P. prepared and discussed the release data. M.S.K. designed experiment and wrote the paper. All authors discussed the results and commented on the manuscript.

Competing financial interests

The authors declare no competing financial interests.

References

[1] M. Horowitz, E. Neeman, E. Sharon, S. Ben-Eliyahu, Exploiting the critical perioperative period to improve long-term cancer outcomes, Nat. Rev. Clin. Oncol. 12 (2015) 213–226.
[2] P.M. Thalanayar, S.S. Agarwala, A.A. Tarhini, Melanoma adjuvant therapy, Chin. Clin. Oncol. 3 (2014) 1–11.
[3] P. Zhang, J. Li, M. Chazwani, W. Zhao, Y. Huang, X. Zhang, et al., Effective co-delivery of doxorubicin and dasatinib using a PEG-Fmoc nanocarrier for combination cancer chemotherapy, Biomaterials 67 (2015) 104–114.
[4] H. Ma, C. He, Y. Cheng, D. Li, Y. Gong, J. Liu, et al., PLK1shRNA and doxorubicin co-loaded thermosensitive PLGA-PEG-PLGA hydrogels for osteosarcoma treatment, Biomaterials 35 (2014) 8723–8734.
[5] P. Papanastasopoulos, J. Stebbing, Molecular basis of 5-fluorouracil-related toxicity: lessons from clinical practice, Anticancer Res. 34 (2014) 1531–1535.
[6] H. Wang, X. Liu, Y. Wang, Y. Chen, Q. Jin, J. Ji, Doxorubicin conjugated phospholipid prodrugs as smart nanomedicine platforms for cancer therapy, J. Mater. Chem. B 3 (2015) 3297–3305.
[7] J. Latchman, A. Guastella, C. Tofthagen, 5-Fluorouracil toxicity and dihydropyrimidine dehydrogenase enzyme: implications for practice, Clin. J. Oncol. Nur 18 (2014) 581–585.
[8] W. Xu, J. Ding, C. Xiao, L. Li, X. Zhuang, X. Chen, et al., Versatile preparation of intracellular-acidity-sensitive oxime-linked polysaccharide-doxorubicin conjugate for malignancy therapeutic, Biomaterials 54 (2015) 72–86.
[9] M. Cheng, Z. Liu, T. Wan, B. He, B. Zha, J. Han, et al., Preliminary pharmacology of galactosylated chitosan/5-fluorouracil nanoparticles and its inhibition of hepatocellular carcinoma in mice, Cancer Biol. Ther. 13 (2012) 1407–1416.
[10] G. Li, Y. Chen, J. Hu, X. Wu, J. Hu, X. He, et al., A 5-fluorouracil-loaded polydioxanone weft-knitted stent for the treatment of colorectal cancer,, Biomaterials 34 (2013) 9451–9461.
[11] M.F. Sorrentino, J. Kim, A.E. Foderaro, A.G. Truesdell, 5-fluorouracil induced cardiotoxicity: review of the literature, Cardiol. J. 19 (2012) 453–458.
[12] A.J. Primeau, A. Rendon, D. Hedley, L. Lilge, I.F. Tannock, The distribution of the anticancer drug doxorubicin in relation to blood vessels in solid tumors, Clin. Cancer Res. 11 (2015) 8782–8788.
[13] M.K. Nguyen, E. Alsberg, Bioactive factor delivery strategies from engineered polymer hydrogels for therapeutic medicine, Prog. Polym. Sci. 39 (2014) 1236–1265.
[14] D.Y. Kim, D.Y. Kwon, J.S. Kwon, J.H. Kim, B.H. Min, M.S. Kim, Injectable in situ–forming hydrogels for regenerative medicines, Polym. Rev. 55 (2015) 407–452.
[15] H. Hyun, S.H. Park, D.Y. Kwon, G. Khang, H.B. Lee, M.S. Kim, Thermo-responsive injectable MPEG-polyester diblock copolymers for sustained drug release, Polymers 6 (2014) 2670–2683.
[16] H.W. Seo, D.Y. Kim, D.Y. Kwon, J.S. Kwon, L.M. Jin, B. Lee, et al., Injectable intratumoral hydrogel as 5-fluorouracil drug depot, Biomaterials 34 (2013) 2748–2757.
[17] Y.M. Kang, G.H. Kim, J.I. Kim, D.Y. Kim, B.N. Lee, S.M. Yoon, et al., In vivo efficacy of an intratumorally injected in situ-forming doxorubicin/poly(ethylene glycol)-b-polycaprolactone diblock copolymer, Biomaterials 32 (2011) 4556–4564.
[18] D.Y. Kim, D.Y. Kwon, H.Y. Seo, J.S. Kwon, B. Lee, D.K. Han, et al., Injectable in situ-forming hydrogels for a suppression of drug burst from drug-loaded microcapsules, Soft Matter 8 (2012) 7638–7648.
[19] B.S. Kim, J.M. Oh, K.S. Seo, J.S. Cho, K.S. Kim, B. Lee, et al., BSA-FITC loaded microcapsules for in vivo delivery, Biomaterials 30 (2009) 902–909.
[20] B.S. Kim, J.M. Oh, H. Hyun, K.S. Kim, S.H. Lee, Y. Kim, et al., Insulin-loaded microcapsules for in vivo delivery, Mol. Pharm. 6 (2009) 353–365.

[21] J. Xu, S. Strandman, J.X.X. Zhu, J. Barralet, M. Cerruti, Genipin-crosslinked catechol-chitosan mucoadhesive hydrogels for buccal drug delivery, Biomaterials 37 (2015) 395–404.
[22] H. Hyun, Y.H. Kim, I.B. Song, J.W. Lee, M.S. Kim, G. Khang, et al., In vitro and in vivo release of albumin using biodegradable MPEG-PCL diblock copolymer as an in situ gel forming carrier, Biomacromolecules 8 (2007) 1093–1100.
[23] M. Iqbal, N. Zafar, H. Fessi, A. Elaissari, Double emulsion solvent evaporation techniques used for drug encapsulation, Int. J. Pharm. 496 (2015) 173–190.
[24] W. Wu, H. Chen, F. Shan, J. Zhou, X. Sun, Z. Zhang, et al., A novel doxorubicin-loaded in situ forming gel based high concentration of phospholipid for intratumoral drug delivery, Mol. Phamaceutics 11 (2014) 3378–3385.